Electronic Supplementary Information (ESI)

A Novel Core-double Shell Heterostructure Derived from Metal-Organic Framework for Efficient HER, OER and ORR Electrocatalysis

Jing Li,[a] Guangshe Li,[a] Jianghao Wang,[a] Chenglin Xue,[a] Xiangshuai Li,[a] Shuo Wang,[a] Bingqi Han,[a] Min Yang[a] and Liping Li*[a]

[a]State Key Laboratory of Inorganic Synthesis and Preparative Chemistry, College of Chemistry, Jilin University, Changchun 130012, PR China.

*E-mail: lipingli@jlu.edu.cn (L. Li)

Content

1. Experimental section

1.1 Chemicals

Cobalt (ll) nitrate hexahydrate ($Co(NO_3)_2 \cdot 6H_2O$), sodium molybdate dehydrate ($(NH_4)_2MoO_4 \cdot 2H_2O$) from Sinopharm Chemical Reagents Co.. Ltd, 2-methylimidazole from Innochem and tioacetamide was purchased from Alfa Aesar. All chemicals were used as received.

1.2 Preparation of Co-Based Metal-Organic Framework ZIF-67:

Cobalt nitrate hexahydrate (1.116 g) and 2-methylimidazole (1.312 g) were dissolved in 30 mL and 10 mL methanol, respectively. Then, the above two solutions were mixed rapidly under fast stirring for 5 min. The obtained suspension was aged for 12 h at room temperature. After that, the precipitate was washed for 3 times by methanol and collected by centrifugation. Finally, the product was dried in vacuum at 80 ^{o}C overnight.

1.3 Preparation of hollow structure of ZIF-67@CoS:

50 mg of ZIF-67 was dispersed in 40 mL of ethanol and the suspension was ultrasonic for 10 min. Then, 50 mg of thioacetamide (TAA) was added and refluxed at 90 ^{o}C for 18 min. After that, the as-obtained product was washed by ethanol for at last 3 times and then dried in vacuum at 60 ^{o}C overnight.

1.4 Preparation of Co@Co_9S_8 nanostructure:

20 mg as-obtained ZIF-67@CoS was annealed in argon atmosphere at 900 ^{o}C for 100 min with a ramp rate of 1 ^{o}C min^{-1}.

1.5 Preparation of Co_9S_8@Co_9S_8@ MoS_2-x (x=0.5, 2.0, 4.0) heterostructure:

Co_9S_8@Co_9S_8@MoS_2-0.5 was synthesized by hydrothermal method. 15 mg Co@Co_9S_8, 7.5 mg sodium molybdate dihydrate and 180 mg L-cysteine was dispersed in 30 mL deionized water. After 15 minutes of ultrasonic dispersion, the mixture then reacted in Teflon-lined stainless steel autoclave of 100 mL at 200 °C for 20 h. Afterwards, the black product was washed by deionized water and ethanol for 5 times and vacuum dried overnight. Finally, the as-obtained product was annealed in Ar/H_2 for 4 h with a ramp rate of 2 °C min^{-1}. The preparation methods of Co_9S_8@Co_9S_8@MoS_2-x (x= 2.0 and 4.0) are similar except that the mass of sodium molybdate dihydrate in Co_9S_8@Co_9S_8@MoS_2-2.0 and Co_9S_8@Co_9S_8@MoS_2-4.0 is 30 mg and 60 mg respectively, where x is the value of MoS_2 mass divide by Co@Co_9S_8 mass. "x" in Co_9S_8@Co_9S_8@MoS_2-x represents mass fraction of m($Na_2MoO_4 \cdot 2H_2O$)/m(Co@Co_9S_8).

1.6 Preparation of MoS_2

MoS_2 was synthesized by hydrothermal method. 60 mg sodium molybdate dihydrate and 180 mg L-cysteine was dispersed in 30 mL deionized water. Before reacting in Teflon-lined stainless steel autoclave of 100 mL at 200 °C for 20 h, the solution should be ultrasonic dispersed for 15 minutes. Afterwards, the black product was washed by deionized water and ethanol for 5 times and vacuum dried overnight. Finally, the as-prepared sample was annealed in Ar/H_2 for 4 h with a ramp rate of 2 °C min^{-1}.

1.7 Preparation of Cobalt phase

20 mg of as-prepared ZIF-67 was annealed in argon atmosphere at 900 °C for 100 min with a ramp rate of 1 °C min^{-1} to obtain Cobalt phase.

1.8 Preparation of Co_9S_8@Co_9S_8@MoS_2-x-mix (x= 0.5, 2.0 and 4.0)

According to results of XRF, we physically mixed Co_9S_8@Co_9S_8 and MoS_2 to prepare Co_9S_8@Co_9S_8@MoS_2-0.5-mix, Co_9S_8@Co_9S_8@MoS_2-2.0-mix and Co_9S_8@Co_9S_8@MoS_2-4.0-mix,

which share the same molar ratios of n(Co_9S_8)/n(MoS_2) with Co_9S_8@Co_9S_8@MoS_2-0.5, Co_9S_8@Co_9S_8@MoS_2-2.0 and Co_9S_8@Co_9S_8@MoS_2-4.0, respectively. In specifically, Co_9S_8@Co_9S_8@MoS_2-0.5-mix was prepared by physically mixing 0.96 mg MoS_2 with 7.68 mg Co_9S_8@Co_9S_8. Similarly, 3.36 mg MoS_2 and 4.64 mg Co_9S_8@Co_9S_8 were mixed in Co_9S_8@Co_9S_8@MoS_2-2.0-mix, 3.76 mg MoS_2 and 4.24 mg Co_9S_8@Co_9S_8 in Co_9S_8@Co_9S_8@MoS_2-4.0-mix. To express more simple, four samples were named as CCM-x-mix (x=0.5, 2.0 and 4.0).

2. Instruments

The powder x-ray diffraction (XRD) patterns were recorded on Rigaku Miniflex apparatus (Cu Kα, λ=1.5418 Å). Scanning electron microscope (SEM) images were characterized using a JSM-6700F. Transmission electron microscopy (TEM), high-angle annular dark field scanning transmission electron microscopy (HAADF STEM) and energy dispersive X-ray spectrometer (EDS) mappings were performed using a Tecnai G2S-Twin F20 apparatus. Chemical compositions were determined with an X-ray fluorescence (XRF) spectrometer (PANalytical, AXIOS). X-ray photoelectron spectroscopy (XPS) spectra were performed on an ESCALAB 250 spectrometer with Mg Kα, radiation. We used C 1s photoemission line at binding energy of 284.6 eV to calibrate all the spectra. Raman spectra were taken at a laser excitation of 532 nm on a Renishaw INVIA Confocal Raman spectrometer. A TriStar 3000 (Micromeritics) nitrogen adsorption apparatus at 77 K were used to record the adsorption-desorption isotherms of N_2 for samples. X-ray absorption near-edge structure (XANES) of S K-edge was performed at the BL12B-a beamline of the National Synchrotron Radiation Laboratory (NSRL).

3. Electrochemical Measurements

3.1 HER and OER Measurements:

Electrochemical measurements were performed in a three-electrode system in conjunction with a CHI 760E workstation (CH Instruments, Inc., Shanghai, China) at room temperature, using Ag/AgCl (KCl, saturated) electrode as the reference electrode, graphite as the counter electrode and glassy carbon electrode of 5 mm diameter (GC) as the working electrode. The GCE was

polished with alpha aluminium oxide powder of 50 nm and washed with deionized water before used. All the potentials were converted to reversible hydrogen electrode (RHE) according to the equation: E (RHE) = E (Ag/AgCl) + 0.059 pH + 0.205 V. 4.0 mg of sample was dispersed in 1 mL of water/alcohol mixed solution with a volume ratio of 9/10 and 50 μL Nafion solution (5%), followed by ultrasonic treatment for 30 min. Then 10 μL of above ink was coated onto GC and dried naturally in air. O_2 or N_2 was saturated in electrolyte by bubbling O_2 or N_2 for 30 min. Linear sweep voltammetry (LSV) was collected at scan rate of 5 mV s^{-1} in N_2 saturated 0.5 mV s^{-1} H_2SO_4 or O_2 or N_2 saturated 1 mol L^{-1} KOH, which is corrected with iR compensation. Cyclic voltammetry (CV) was used to access double-layer capacitance, which was tested with different scan rate (40, 80, 120, 160 and 200 mV s^{-1}) at 1.31-1.41 V (vs. RHE). Chronopotentiometry measurement was carried at the potential related to ~10 mA cm^{-2}. Electrochemical impedance spectrum (EIS) was performed at -0.10 V for N_2-saturated 1 mol L^{-1} KOH, for N_2-saturated 0.5 mol L^{-1} H_2SO_4 and -0.29 V for O_2-saturated 1 mol L^{-1} KOH. Specific activity (mA cm^{-2}) was based on BET surface area and calculated according to the formula: Specific Activity = $j/(10 \times S_{BET} \times m)$, where m fixed at 0.2 mg cm^{-2}.

3.2 ORR Measurements:

Electrochemical measurements were carried on a CHI 760E workstation with three-electrode system in O_2-saturated 0.1 mol L^{-1} KOH at room temperature, with a GC RDE (5 mm in diameter) serving as work electrode, Ag/AgCl (KCl, saturated) electrode as the reference electrode and Pt wire as the counter electrode.

The pre-catalyst ink were prepared by mixing 4 mg of sample, 495 μL of water, 500 μL alcohol and 5 μL Nafion solution (5%), following by ultrasonic treatment for 30 min to form homogeneous ink. Then a certain volume of above ink was coated onto GC with the loading of nonprecious pre-catalyst was 0.40 mg cm^{-2} and that of Pt/C was 0.2 mg cm^{-2}, dried naturally in air. N_2 or O_2 flow was bubbled for 30 min before tests to achieve N_2 or O_2 saturated solution. The CV tests were measured at potential window of 0.17-0.92 V with a rate of 50 mV s^{-1} in O_2- or N_2- saturated 0.1 mol L^{-1} KOH. LSV was conducted on RDE/RRDE with sweep rate of 10

mV s^{-1} at different rotation rates in O_2-saturated 0.1 mol L^{-1} KOH. The durability tests were performed at 0.6 V vs. RHE for 12 h in O_2-saturated 0.1 mol L^{-1} KOH. The following two equations are used to calculate the hydrogen peroxide yield (H_2O_2%) and the electron transfer number (n).

$$H_2O_2(\%) = 200 \times \frac{\frac{I_r}{N}}{I_d + \frac{I_r}{N}}$$

$$n = 4 \times \frac{I_d}{I_d + \frac{I_r}{N}}$$

Where I_d is the disk current, I_r is the ring current and N=0.37 is the ring collection efficiency.

Koutecky-Levich plot based on Koutecky-Levich equations can be used to calculate electron transfer number (n) and kinetic current density (J_k).

$$\frac{1}{J} = \frac{1}{J_L} + \frac{1}{J_K} = \frac{1}{B\omega^{\frac{1}{2}}} + \frac{1}{J_K}$$

$$B = 0.62nFC_0D_0^{\frac{2}{3}}V^{-\frac{1}{6}}$$

$$J_K = nFkC_0$$

Where J, J_K and J_L are the measured current density, the kinetic and limiting current densities, respectively, ω is the angular velocity of the disk electrode, n is the electron transfer number, F is the Faraday constant (96485 C mol^{-1}), C_0 is the bulk concentration of O_2 (1.2×10^{-6}mol cm^{-3}), D_0 is the diffusion coefficient of O_2 in 0.1 mol L^{-1} KOH ($1.9\times10^{-5}cm^2s^{-1}$), and V is the kinematic viscosity of the electrolyte (0.01 cm^2s^{-1}).

4. Characterizations

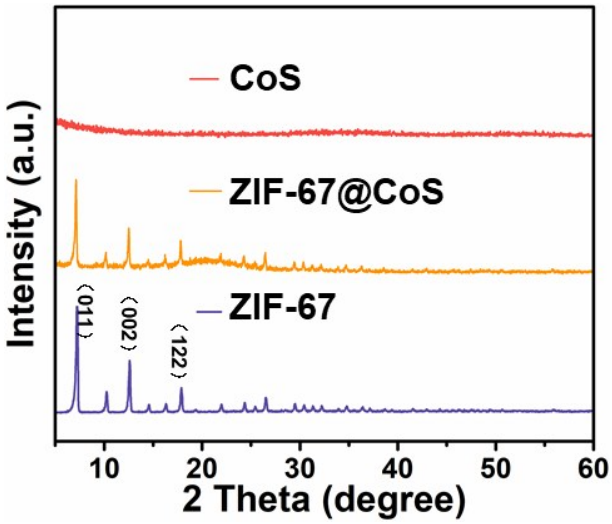

Fig. S1 XRD patterns of ZIF-67, ZIF-67@CoS and CoS.

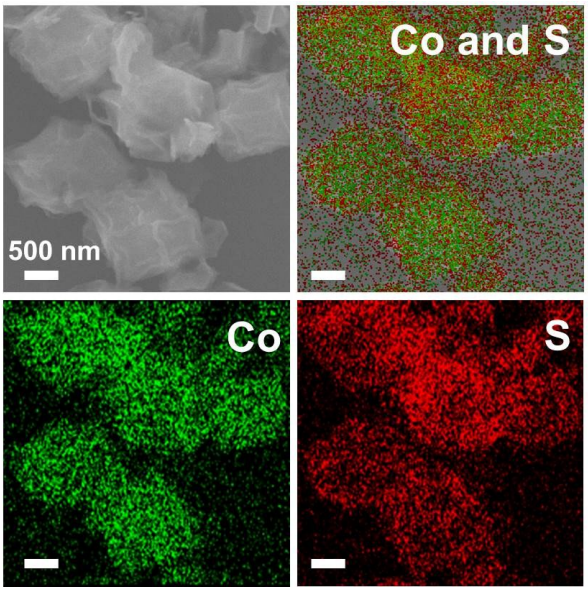

Fig. S2 EDS mapping of Co and S elements for ZIf-67@CoS sample.

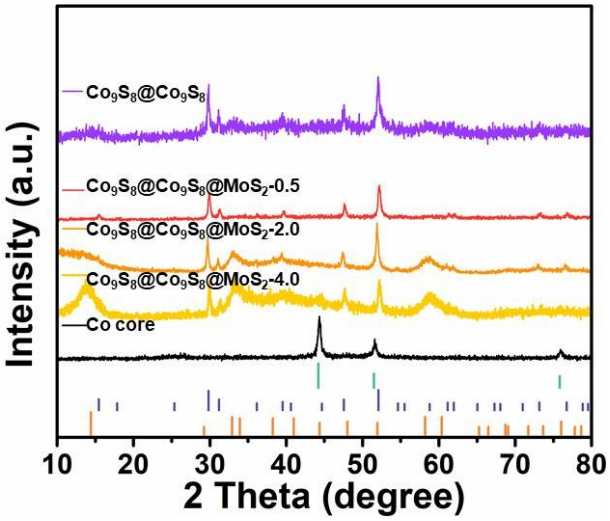

Fig. S3 XRD patterns of Co_9S_8@Co_9S_8, Co_9S_8@Co_9S_8@MoS_2-0.5, Co_9S_8@Co_9S_8@MoS_2-2.0, Co_9S_8@Co_9S_8@MoS_2-4.0, Co@C and corresponding standard patterns of Co (JCPDS No. 15-0806) (green line), Co_9S_8 (JCPDS No. 73-1442) (purple line), MoS_2 (JCPDS No. 17-0744) (orange line).

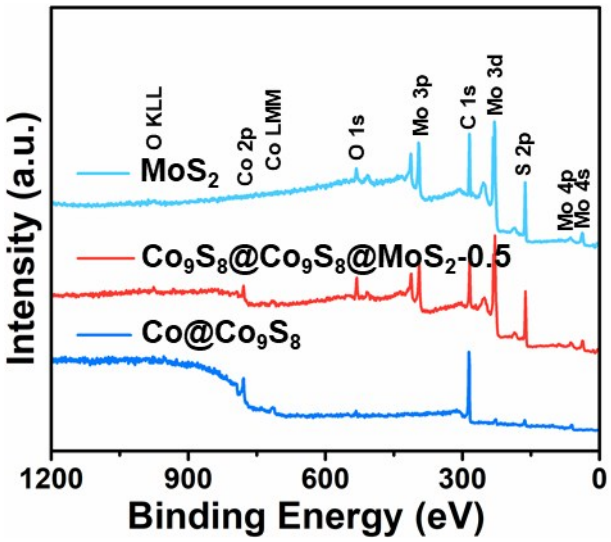

Fig. S4 XPS survey spectra of Co_9S_8@Co_9S_8@MoS_2-0.5, Co@Co_9S_8 and MoS_2.

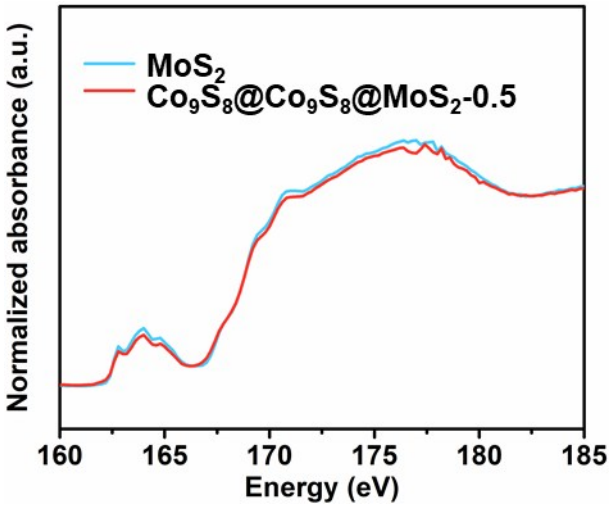

Fig. S5 S L-edge XANES spectra of Co_9S_8@Co_9S_8@ MoS_2-0.5 and MoS_2.

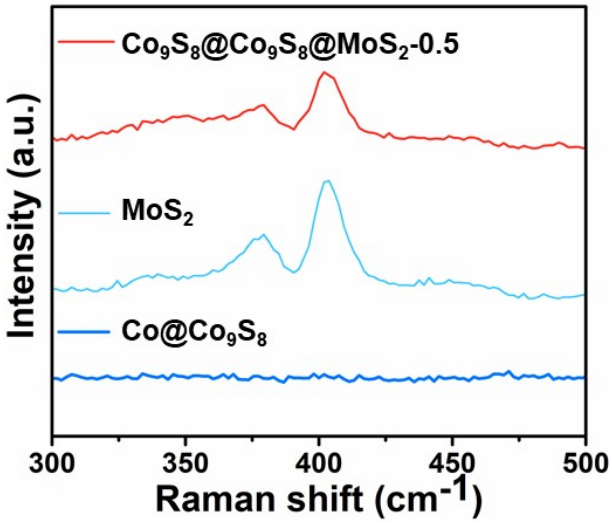

Fig. S6 Raman spectra of Co_9S_8@Co_9S_8@ MoS_2-0.5, Co@Co_9S_8, and MoS_2.

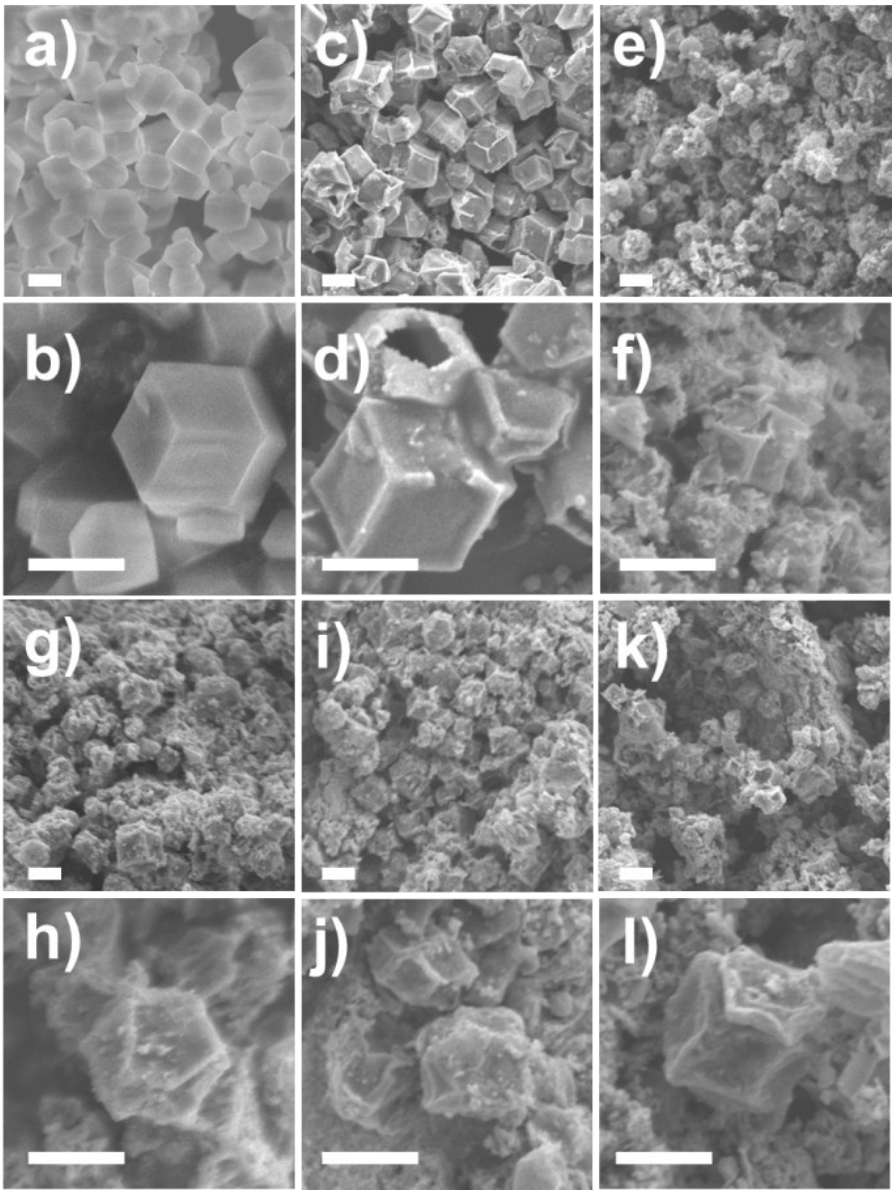

Fig. S7 SEM images of a) and b) ZIF-67; c) and d) ZIF-67@CoS; e) and f) Co@Co_9S_8; g) and h) Co_9S_8@Co_9S_8@ MoS_2-0.5; i) and j) Co_9S_8@Co_9S_8@ MoS_2-2.0; k) and l) Co_9S_8@Co_9S_8@ MoS_2-4.0 (scale bar is 200 nm).

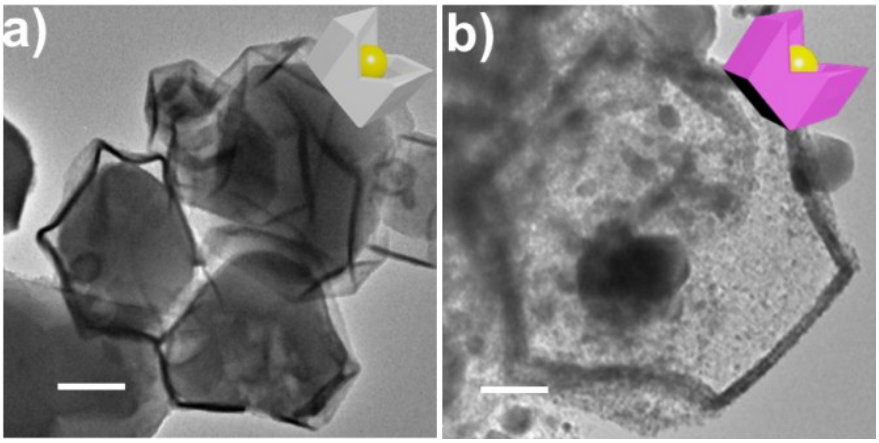

Fig. S8 TEM images of a) ZIf-67@CoS and b) Co@Co_9S_8 (Scale bar = 100 nm).

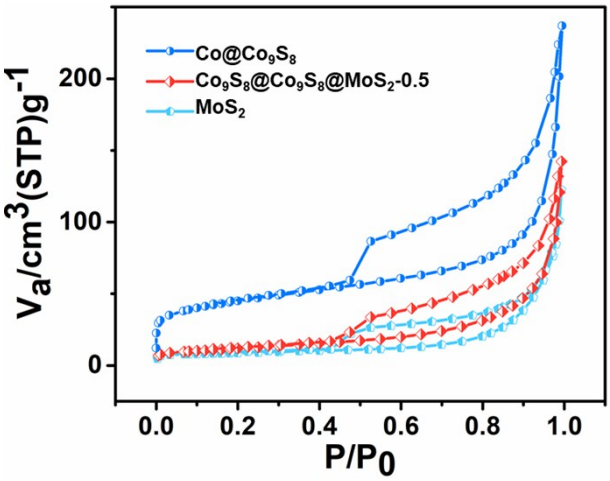

Fig. S9 N_2 sorption isotherm of Co@Co_9S_8, Co_9S_8@Co_9S_8@ MoS_2-0.5 and MoS_2.

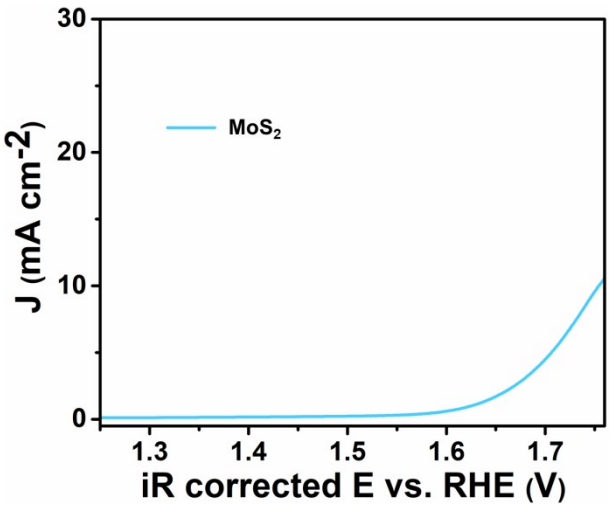

Fig. S10 LSV curves of MoS_2 tested in 1 mol L^{-1} O_2-saturated KOH.

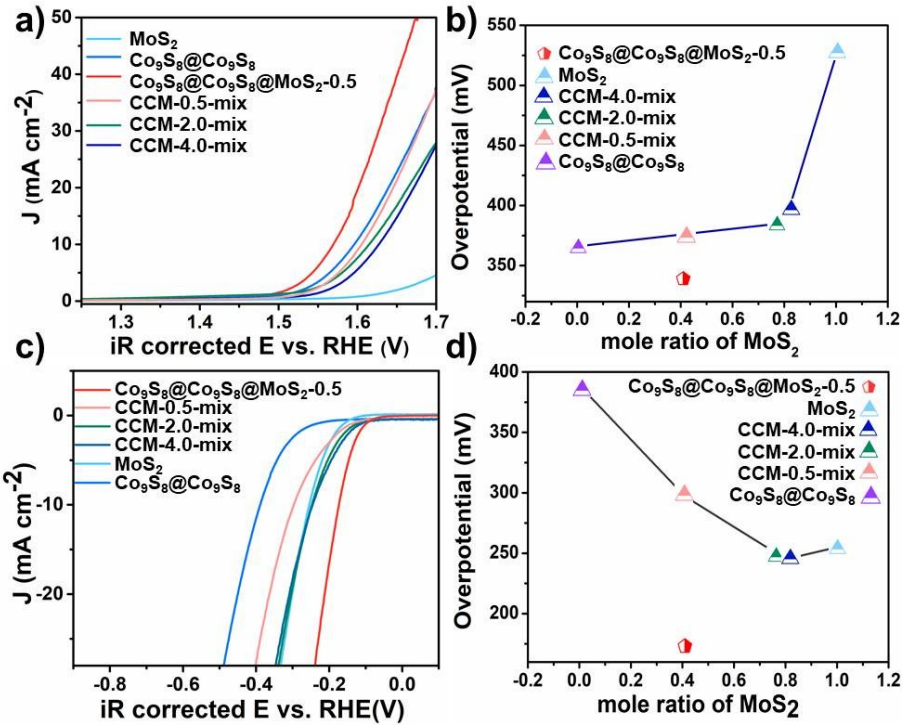

Fig. S11 a) LSV curves of MoS_2, Co_9S_8@Co_9S_8, CCM-0.5-mix, CCM-2.0-mix, CCM-4.-mix and Co_9S_8@Co_9S_8@MoS_2-0.5 tested in 1 mol L^{-1} O_2-saturated KOH; b) Plot of potential vs. mole ratio of MoS_2 for OER; c) LSV curves of MoS_2, Co_9S_8@Co_9S_8, CCM-0.5-mix, CCM-2.0-mix, CCM-4.-mix and Co_9S_8@Co_9S_8@MoS_2-0.5 tested in 1 mol L^{-1} H_2-saturated KOH; d) Plot of potential vs. mole ratio of MoS_2 for HER.

As illustrated in Fig. S11b and S11d, the plots of overpotential vs. mole ratio of MoS_2 show obviously non-linear. Specifically, overpotential of MoS_2 for OER is 525 mV at 10 mA cm^{-2} and gradually decreases with increasing the amount of Co_9S_8@Co_9S_8 in the mixture. As a result, overpotentials of CCM-4.0-mix, CCM-2.0-mix and CCM-0.5-mix for OER are calculated to be 398, 385 and 375 mV respectively, which are gradually close to pure Co_9S_8@Co_9S_8 (366 mV). Overpotential vs. mole ratio of MoS_2 plot for HER is similar with that for OER. Composition and synergistic effect among components could change overpotential of physical mixtures for OER and HER reaction. Therefore,

the obviously non-linear plot (potential vs. mole ratio of MoS_2) demonstrated the presence of synergistic effect between Co_9S_8@Co_9S_8 and MoS_2.

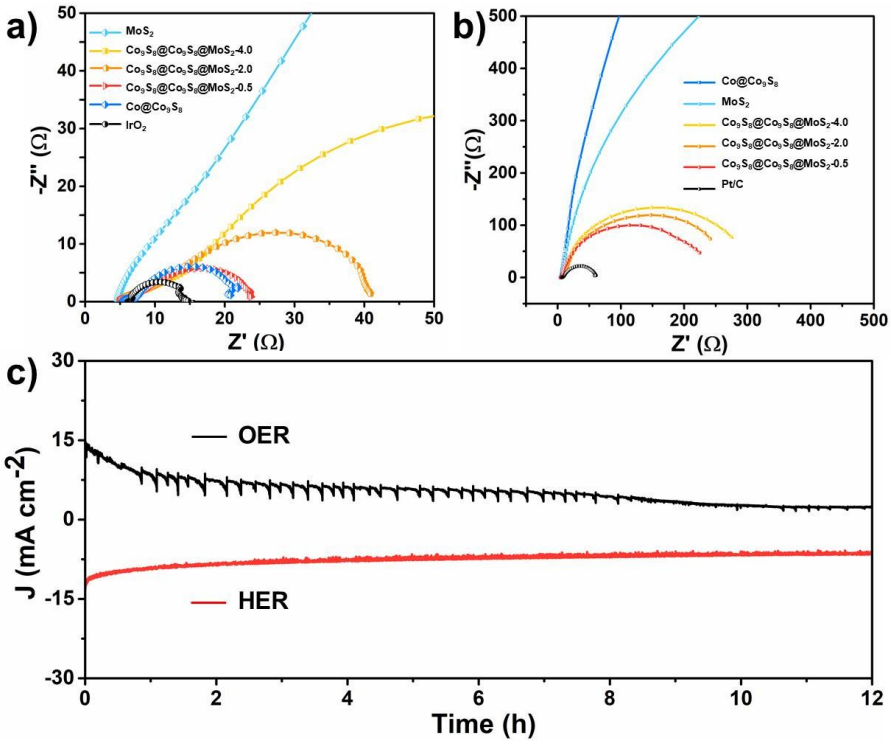

Fig. S12 Nyquist plots of pre-catalysts a) recorded at -0.09 V vs. RHE in N_2-saturated 1 mol L^{-1} KOH; b) recorded at 1.57 V vs. RHE in O_2-saturated 1 mol L^{-1} KOH; c) stability test for HER recorded at -0.20 V and OER recorded at 1.59 V. The semicircular diameter at high frequencies in (a) and (b) plots are the charge transfer resistances (R_{ct}) of samples.

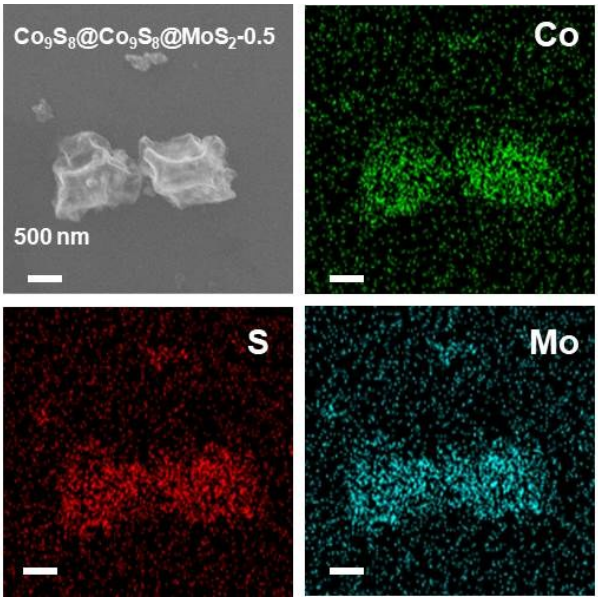

Fig. S13 EDS mapping of Co, Mo, S elements of Co_9S_8@Co_9S_8@MoS_2-0.5 after HER stability test at -0.2 V vs. RHE for 12 hours.

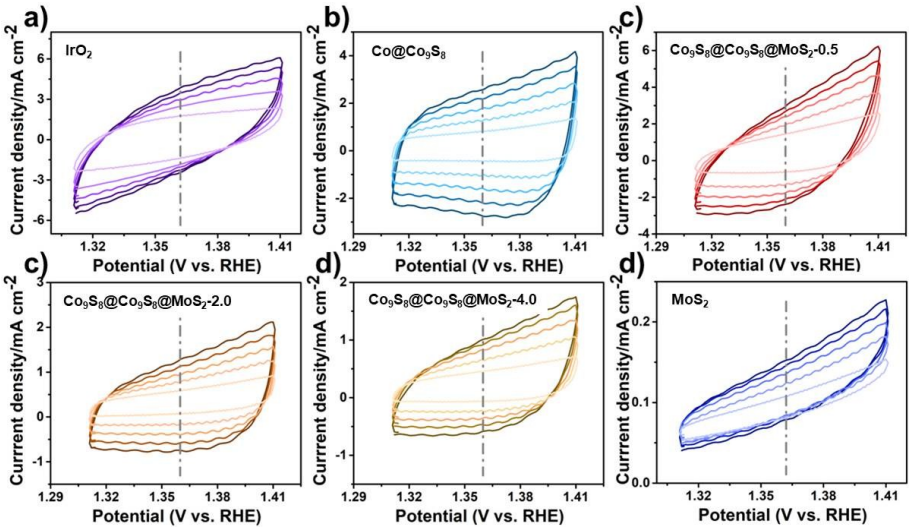

Fig. S14 Electrochemical double layer capacitance curves of a) IrO_2; b) Co@Co_9S_8; c) Co_9S_8@Co_9S_8@ MoS_2-0.5; d) Co_9S_8@Co_9S_8@ MoS_2-2; e) Co_9S_8@Co_9S_8@MoS_2-4 and f) MoS_2 with different scan rates.

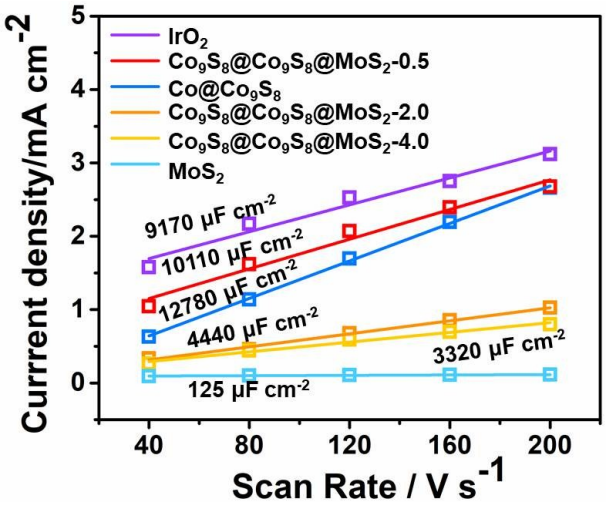

Fig. S15 Plots of current densities at 1.36 V versus scan rates of samples.

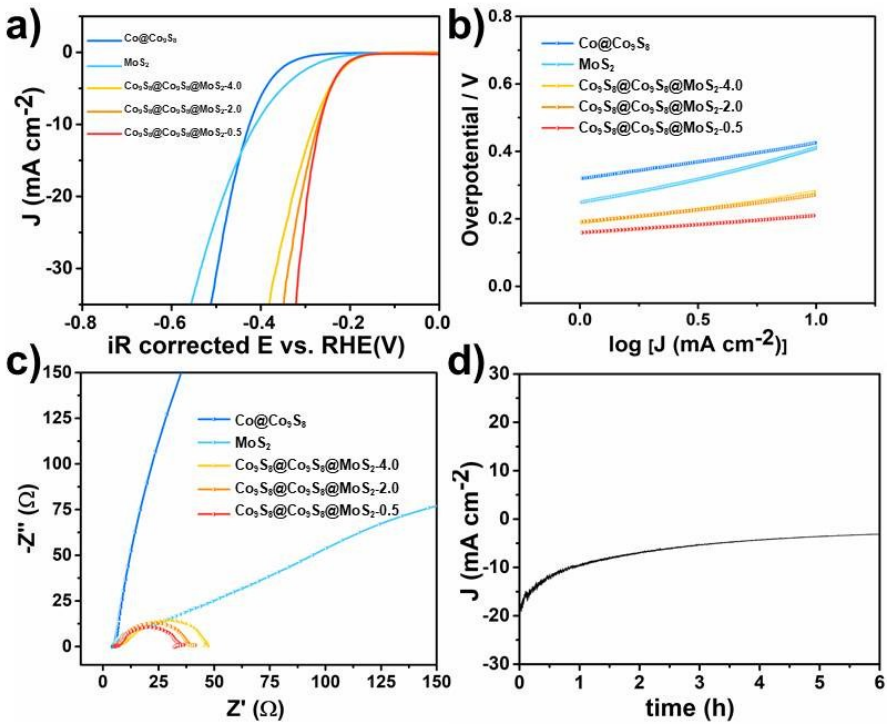

Fig. S16 HER performance of Co@Co_9S_8, Co_9S_8@Co_9S_8@MoS_2-0.5, Co_9S_8@Co_9S_8@MoS_2-2, Co_9S_8@Co_9S_8@MoS_2-4 and MoS_2 a) LSV curves tested in N_2-saturated 0.5 mol L^{-1} H_2SO_4 (scan rate 5

mV s^{-1}); b) Tafel slops, c) Nyquist plots of pre-catalyst recorded at -0.255 V vs. RHE; and d) the current density-time curve of Co_9S_8@Co_9S_8@MoS_2-0.5 tested at -0.315 V vs. RHE for 6 h.

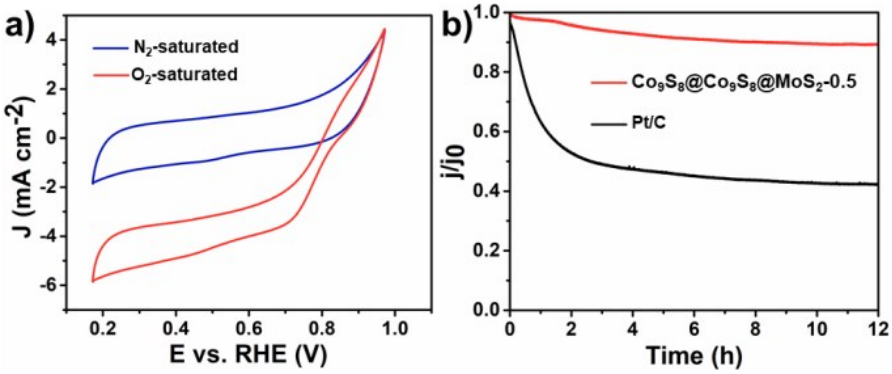

Fig. S17 a) CVs of Co_9S_8@Co_9S_8@MoS_2-0.5 in O_2- and N_2- saturated 0.1 mol L^{-1} KOH; and b)The i-t curves of Co_9S_8@Co_9S_8@MoS_2-0.5 and Pt/C tested at 0.6 V for 12 hours.

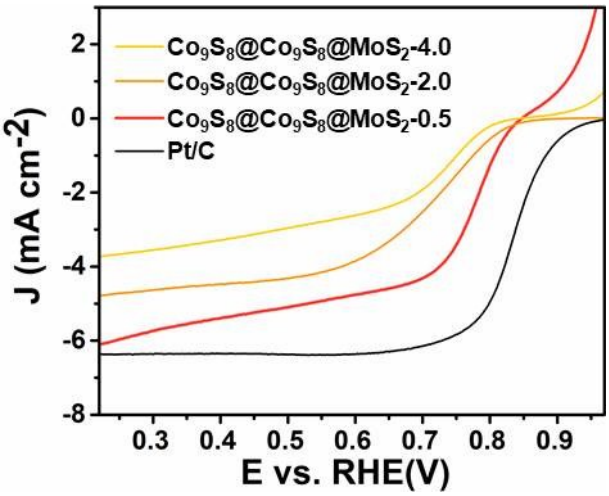

Fig. S18 RDE polarization curves of Co_9S_8@Co_9S_8@MoS_2-0.5, Co_9S_8@Co_9S_8@MoS_2-2.0, Co_9S_8@Co_9S_8@MoS_2-4.0 and Pt/C tested in O_2-saturated 0.1 mol L^{-1} KOH with a sweep rate of 10 mV s^{-1} at 1600 rpm.

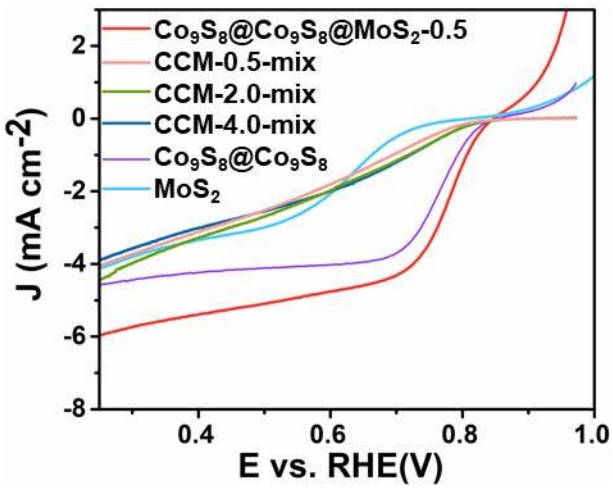

Fig. S19 RDE polarization curves of CCM-0.5-mix, CCM-2.0-mix, CCM-4.0-mix and Pt/C tested in O_2-saturated 0.1 mol L^{-1} KOH with a sweep rate of 10 mV s^{-1} at 1600 rpm.

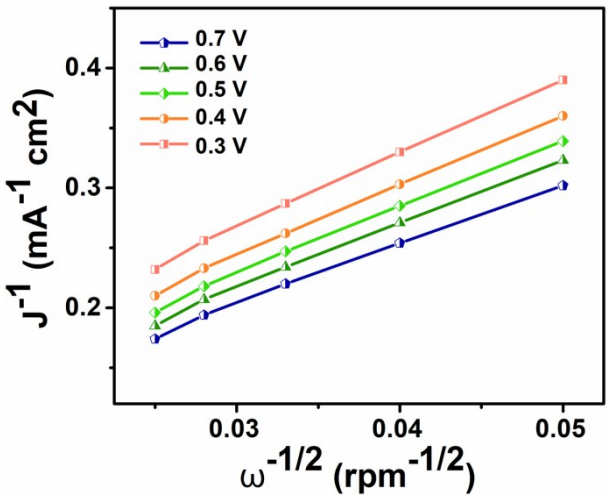

Fig. S20 Koutecky-Levich plots (J^{-1} versus $\omega^{-0.5}$) at different potentials.

Table S1. Composition of Co_9S_8@Co_9S_8@MoS_2-0.5, Co_9S_8@Co_9S_8@MoS_2-2.0 and Co_9S_8@Co_9S_8@MoS_2-4.0 characterized by X-ray fluorescence.

Sample	Atomic ratio of Co/Mo	Mole ratio of MoS_2 to Co_9S_8
Co_9S_8@Co_9S_8@MoS_2-0.5	1/0.0767	0.41
Co_9S_8@Co_9S_8@MoS_2-2.0	1/0.401	0.78
Co_9S_8@Co_9S_8@MoS_2-4.0	1/0.491	0.82

Table S2. C wt.%, N wt.% and H wt.% obtained by CHNS elemental analysis

Samples	C wt.%	N wt.%	H wt.%
Co_9S_8@Co_9S_8@MoS_2-0.5	6.80	0.16	3.07
Co_9S_8@Co_9S_8@MoS_2-2.0	4.55	0.15	2.03
Co_9S_8@Co_9S_8@MoS_2-4.0	3.53	0.09	2.11